INTERNATIONAL ATOMIC ENERGY AGENCY
UNITED NATIONS EDUCATIONAL, SCIENTIFIC AND CULTURAL ORGANIZATION
INTERNATIONAL CENTRE FOR THEORETICAL PHYSICS
I.C.T.P., P.O. BOX 586, 34100 TRIESTE, ITALY, CABLE: CENTRATOM TRIESTE

H4-SMR 471/22

COLLEGE ON MEDICAL PHYSICS

10 - 28 SEPTEMBER 1990

MAGNETIC RESONANCE DOSIMETRY: STATE OF THE ART AND FUTURE DEVELOPMENTS

O. Baffa

Universidade de Sao Paulo
Sao Paulo
Brazil

MAGNETIC RESONANCE DOSIMETRY: STATE OF THE ART AND FUTURE DEVELOPMENTS

Oswaldo Baffa
Physics Department
Faculdade de Filosofia Ciencias e Letras de Ribeirão Preto
Universidade de São Paulo
Av. Bandeirantes, 3900
14049-Ribeirão Preto-SP, Brazil

Abstract

A review of magnetic resonance applied to detect and measure the effects of ionising radiation is made. Examples of the use of Electron Spin Resonance and Nuclear Magnetic Resonance for dosimetric purposes in medical physics are presented.

Contents

1 Introduction

Magnetic Resonance Dosimetry (MAGDOS) could be classified as a kind of chemical dosimetry since what is measured are the stable free radicals that ultimately are the result of some broken chemical bonds. However the complexity involved in the interpretation and measurement in MAGDOS justifies treatment separate from the conventional chemical dosimetry such as Fricke Dosimetry.

Until very recently, the subject of MAGDOS was restricted to the application of Electron Spin Resonance (ESR) to measure of spin concentration as a function of the dose absorbed in samples that have been irradiated. Another way to assess the effects of the dose on matter is by measuring the changes in relaxation times of a nuclear spin system due to the paramagnetism produced by the radiation of molecules or ions. With the advent of magnetic resonance imaging scanners the effect of the radiation on the relaxation properties of the material can be exploited to produce images of a phantom contrasted by the relaxation time that give a quick information about the spatial deposition of the dose in the phantom.

The presentation of this topic will begin with a description of the paramagnetism exhibited by electrons. Then the basic principles of the magnetic resonance phenomenon will be discussed for the case of electrons and protons, namely electron spin resonance (ESR) and nuclear magnetic resonance (NMR), followed by examples and applications of these two phenomena. The applications will be selected according to their relevance to medical physics. The magnetic resonance theory that will be developed will be quite elementary and the reader should consult the books of Poole & Farach [42], Pake [41],Slichter [51] and Farrar [22] for more details on the fundamentals of the theory of ESR and NMR.

2 Electronic Paramagnetism

The magnetic resonance phenomenon appears in systems of particles having angular momentum J. This may be both from orbital (L) and spin (S) motion. The former is important for the transitions ions, except for iron in which the crystal fields quench the effects of the orbital motion. For an ensemble of free electrons,the main concern in these lectures, only the spin has to be taken into account to derive the magnetic properties of the system.

The magnetic moment associated with a free electron having spin S can be written as:

$$\mu = g(eh/2mc)S = -g\beta S = -\gamma hS \qquad (1)$$

where the constants are defined as follows: $\beta = eh/2mc = 0.927310^{-20}$ erg/gauss is the Bohr magneton, g is the spectroscopic splitting factor which

for a free electron is equal to 2.0023 and γ is the gyromagnetic ratio equal to $2.8025\,MHz/G$.

Now suppose that we apply a static magnetic field $H_o = H_o\hat{k}$ to a system of free electrons and then ask how big the macroscopic magnetization will be. Energy will build up in the system and for an individual electron we have:

$$E_i = -\mu_i H_o = -g\beta H_o S_z = g\beta H_o m_i \tag{2}$$

where m_i are the spin quantum numbers that have the values of $\pm 1/2$ for a free electron and correspond to the only allowed transitions. From equation 2 electrons in a magnetic field can have two energies, namely

$$E_+ = +1/2gH_o \tag{3}$$

$$E_- = -1/2gH_o \tag{4}$$

which correspond to the spin antiparalell and parallel to H_o, respectively.

The energies above could be obtained by a rigorous calculation using the Zeeman Hamiltonian of a spin in a magnetic field:

$$\mathcal{H} = \beta\vec{H}\cdot\tilde{g}\cdot\vec{S} \tag{5}$$

where the $\tilde{g}$ is now a tensor.

The probability of having a magnetic moment aligned with the magnetic field will be given by the Boltzmann factor normalized by the probability of finding μ in any direction. Thus the magnetization in the z direction can be written as:

$$M_z = 1/v\sum\mu_{zi} = g\beta\frac{(N_+ - N_-)}{(N_+ + N_-)} = g\beta\frac{N}{2}\frac{1-exp(-g\beta H/kT)}{1+exp(-g\beta H/kT)} \tag{6}$$

where N is the total number of paramagnetic centers per unit volume and N_+, N_- are the density of spins pointing parallel and antiparallel to the magnetic field. Expression 6 is cumbersome and usually a simplification is made if the argument $g\beta H_o/2kT \ll 1$, the so-called high temperature approximation. We have

$$M_z = \frac{Ng^2\beta^2 H}{4kT} \tag{7}$$

Expression 7 can be generalized for spins other than 1/2 giving:

$$M_z = \frac{Ng^2\beta^2[S(S+1)]H_o}{3kT} \tag{8}$$

which corresponds to the Curie law for the static susceptibility $\chi_o = M/H_o$. However for the typical values of fields employed in ESR the term $g\beta H_o/2K \simeq 1K$ which is by no means a high temperature. Thus the expansion must retain terms beyond the first one.

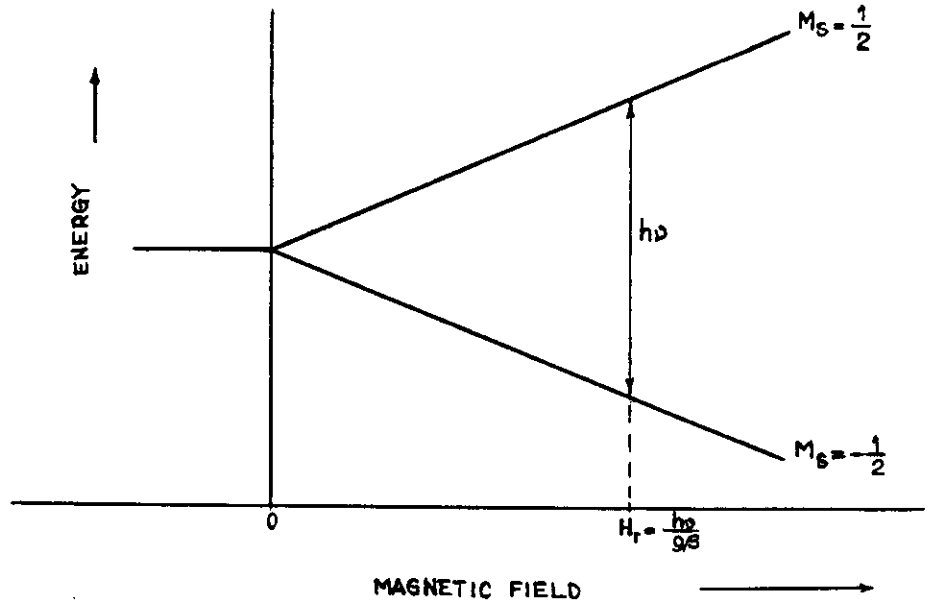

Figure 1: Energy splitting as a function of the magnetic field

Expressions 3 and 4 tell us that for zero external field H_o the Zeemmann energies are zero and they change linearly with the field as shown in figure 1. Two energy levels are created such that transitions may be induced if a quantum

$$\Delta E = h\nu = g\beta H \tag{9}$$

is provided by appropriate means. In order for this transition to occur a non zero matrix element connecting the two states must exist. This is made possible if a small oscillating field H_1 at the frequency ν is applied perpendicularly to H_o. When condition 9 is satisfied the system is said to be in resonance.

Electron Spin Resonance is a spectroscopic technique that measures the amount of energy absorbed in this way by the spin system. For practical fields obtained in the laboratory the frequency ν is on the order of GHz, the so-called microwave region of the electromagnetic spectrum.

According to the transition probability expressions the same field frequency that flips the spin up (antiparallel to the field) will with the same probability flip it down. Thus is it really possible to detect any net energy absorption ? The answer is yes and to understand why we must bring to the scene an important partner, the lattice. Lattice here is to be understood as a heat reservoir from which energy may be exchanged. In this context it does not have to be an organized array of atoms as is the case for a crystal.

Defining $n = N_- - N_+$ as the difference in population, we may write an equation for the time variation of n that results from the combined action of the microwave field and the lattice on the spin system:

$$\left(\frac{dn}{dt}\right) = \left(\frac{dn}{dt}\right)_{\mu w} + \left(\frac{dn}{dt}\right)_{latt} \tag{10}$$

The first term is the variation produced by the microwave field and since $<+|v|->^2=<-|v|+>^2$, where v is the operator corresponding to the microwave field H_1, it can be written as:

$$\left(\frac{dn}{dt}\right)_{\mu w} = \left(\frac{dN_-}{dt}\right) - \left(\frac{dN_+}{dt}\right) = P(N_+ - N_-) - P(N_- - N_+) = 2Pn \tag{11}$$

The interaction with the lattice can be described as an exponential exchange of energy:

$$\left(\frac{dn}{dt}\right)_{latt} = \frac{n_o - n}{T_1} \tag{12}$$

where T_1 is a characteristic time known as the spin lattice relaxation time . Inserting expressions 11a and 12 into expression 10 we get:

$$\left(\frac{dn}{dt}\right) = \frac{-2Pn + n_o - n}{T_1} \tag{13}$$

In the steady state dn/dt in expression 13 is equal to zero and we have:

$$n = n_o\left(\frac{1}{1+2PT_1}\right) \tag{14}$$

From expression 14 we see that the population difference goes to zero if $PT_1 \gg 1$ and no energy absorption will be detected. This condition is known as saturation and must be avoided experimentally by varying P and T_1 by changing the temperature of the sample.

3 The Classical View of Magnetic Resonance

The notion of mechanical resonance is common to us. Examples of an automobile with unbalanced wheels that begin to vibrating at a certain speed (angular frequency), a child being pushed in a swing or the collapse of the Tacoma bridge come to mind when we think about resonance. It is useful, although not fully precise, to imagine the magnetic resonance phenomenon also in classical terms.

Suppose that we have a magnetic moment making an angle α with the magnetization as shown in figure 2. Since the energy of the magnetic moment is a function of the angle α, the magnetization can precess around H_o, like a top precessing around the earth's gravitational field. The precession frequency can be deduced by writing the equation of motion for the magnetization as follows:

$$\frac{d\vec{M}}{dt} = \gamma(\vec{M} \times \vec{H}_O) \tag{15}$$

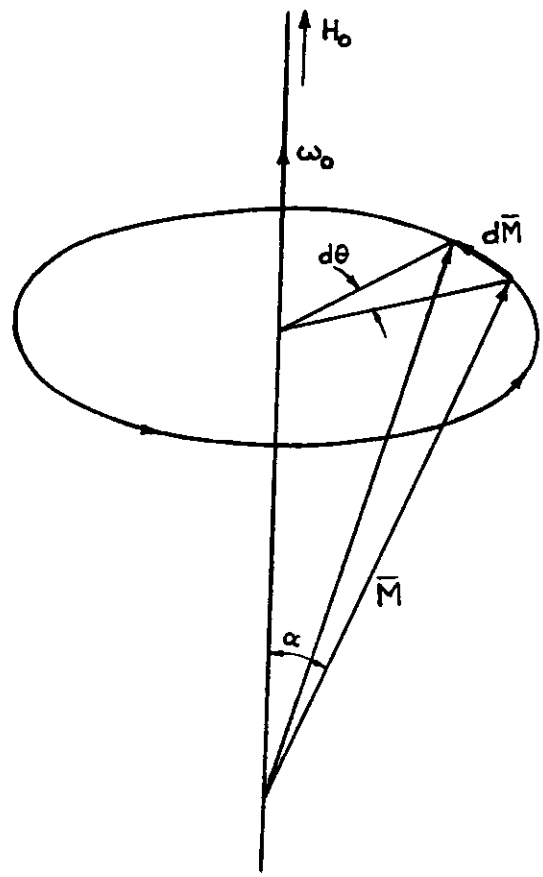

Figure 2: Vector magnetization $\vec{M}$ precessing in a static magnetic field H_o.

The ingredients to deduce the precession Larmor frequency ω_o are indicated in figure 2:

$$\vec{\omega}_o = \gamma \vec{H}_o \tag{16}$$

In order to change the angle α a magnetic field H_1 perpendicular to H_o, has to be applied. If this field oscillates with the frequency ω_o and the correct phase it causes the system to enhance the energy in the same way as when we push a swinging child. The time of action of this field will determine the angle formed with H_o and a continuous irradiation of the sample will lend the net magnetization antiparlallel relative to field, that after some time will relax to the original orientation.

Felix Bloch proposed a set of equations to describe the motion of the macroscopic magnetization. They are valid under the assumption that $H_1 \ll H_o$ and in laboratory system of axis are written as:

$$\frac{dM_x}{dt} = \gamma(\vec{H} \times \vec{M})_x - \frac{M_x}{T_2} \tag{17}$$

$$\frac{dM_y}{dt} = \gamma(\vec{H} \times \vec{M})_y - \frac{M_y}{T_2} \tag{18}$$

$$\frac{dM_z}{dt} = \gamma(\vec{H} \times \vec{M})_z - \frac{(M_o - M_z)}{T_1} \tag{19}$$

where the M_x,M_y and M_z are the components of the magnetization along the x,y and z directions. T_1 is the spin lattice relaxation time and T_2 is the spin-spin relaxation time. As discussed before T_1 is related with the change of the magnetization along the z direction. T_2 is related with the destruction of magnetization perpendicular to H_o and has to do with the fact that the spins experience slightly different dipolar fields from their neighbors. Having different Larmor frequencies they start to precess in the perpendicular plane incoherently, leading to a loss of M_x and M_y.

Equations 19 17 18 can be solved for an oscillatory field of the form:

$$H_x = 2H_1 \cos \omega t \tag{20}$$

The oscillating field will induce an oscillating complex susceptibility, where χ' the real amplitude is called the dispersion and the imaginary amplitude χ'' is the absorption term. The magnetization induced by H_1 can be written as:

$$M_x = 2\chi' H_1 \cos \omega t + 2\chi'' H_1 \cos \omega t \tag{21}$$

Solving Bloch equations and comparing with expression 21 we obtain χ' and χ'' as follows:

$$\chi' = \frac{\chi_o T_2 \omega_o}{2} \left(\frac{T_2(\Delta\omega)}{1 + T_2^2(\Delta\omega)^2 + \gamma^2 H_1^2 T_1 T_2} \right) \tag{22}$$

$$\chi'' = \frac{\chi_o T_2 \omega_o}{2}\left(\frac{1}{1+T_2^2(\Delta\omega)^2+\gamma^2 H_1^2 T_1 T_2}\right) \tag{23}$$

In equation 22 $\Delta\omega$ is the difference between the actual and the resonance frequencies. Since what is measured in a magnetic resonance experiment is the power absorbed from the microwave field that establishes H_1 by the spin system when it changes from the low energy level, parallel to H_o, to the high energy level, antiparallel to H_o, let us use the classical model to calculate the average power, in a period T, absorbed by the magnetization induced by the oscillating field H_1. The following expression can be written for the energy of a magnetization in a magnetic field:

$$P = \frac{1}{T}\int_0^T \vec{H}\cdot d\vec{M} \tag{24}$$

Substituting $\vec{M}$ and $\vec{H}$ in expression 24 and carrying out the integration we get the net power absorbed per cycle as:

$$P = \frac{1}{2}\omega\chi''(2H_1)^2 \tag{25}$$

Substitution of χ'' on equation 25 and comparison with equation 14 from the previous section gives the saturation parameter P as:

$$P = \frac{1}{2}(\gamma H_1)^2 T_2 \tag{26}$$

This result is the same as the one obtained from exact quantum mechanics calculations.

4 Hyperfine Interaction

So far we have talked about the interaction of an electron with an external magnetic field H_o, or Zeeman interaction. Electrons can also interact with the magnetic moments of neighbor nuclei in what is called hyperfine interaction. This interaction can be divided in two contributions: One part is anisotropic due to the interaction of the electron and nuclear magnetic moment and can be written in the same way as two interacting magnetic dipoles $\vec{\mu_1}$ and $\vec{\mu_2}$. The other part is isotropic and has no classical analog. It is due to the finite probability of finding the electron on the nucleus (Fermi contact interaction). For powder and frozen solution samples the anisotropic contribution averages to zero and only the isotropic part contributes to the hyperfine interaction. The Hamiltonian 5 can be written now to include the nuclear interaction as follows:

$$\mathcal{H} = -g\beta\vec{S}\cdot\vec{H} + A\vec{S}\cdot\vec{I} + g_N\beta_N\vec{I}\cdot\vec{H} \tag{27}$$

In this expression the term A represents the hyperfine interaction and we include also the nuclear Zeeman interaction (last term). $\vec{I}$ is the nuclear spin, g_N is the nuclear g factor and β_N is the nuclear magneton.

The energies can be written as:

$$E = g\beta_o m_S + A m_S m_I - g_N \beta_N H_o m_I \tag{28}$$

Here m_S and m_I are the electronic and nuclear quantum numbers. Since the electron mass is much less than the nuclei mass, the magneton for the nucleus is much smaller than the electronic and we can neglect the last term when studying electronic transitions. Consider a simple case when $S = \frac{1}{2}$ and $I = \frac{1}{2}$. Now the energy levels obtained previously by equation 2 will be modified because for each electronic level there is a possibility of having the nuclear moment adding or subtracting a small field from the static field H_o and the previous levels will be displaced a little bit up and down as shown in figure 3. Now instead of only one allowed transition we can have two, with the selection rules $\Delta m_S = \pm 1$ and $\Delta m_I = 0$. The distance between the peaks is A and the center of the spectrum determines the g factor. A spectrum with resolved hyperfine lines is very useful in the identification of the paramagnetic species under study.

5 The ESR Spectrometer

Figure 4 shows the basic components of an ESR spectrometer. Electromagnetic microwaves are produced by a Klystron or Gunn oscillator and directed to a magic T trough waveguides or strip lines. Magic T can be thought as the microwave analog of a Wheatstone bridge. The microwaves are divided in the magic T in one part that goes to the sample cavity and in another part that goes to the reference arm. After being reflected by the sample in the cavity and by the reference arm the waves will interfere and are directed to the detector, usually a diode. The sample cavity is resonant at a fixed frequency and this enhances the oscillating magnetic field H_1 at certain cavity positions where the sample is inserted. The phase shifter in the reference arm allows the detection of the real (χ') and imaginary parts (χ'') of the magnetic susceptibility since they are 90° out of phase.

The resonant cavity is inserted in a gap of an electromagnet to produce the static field H_o, typically 5kG for a resonant frequency of 9 GHz (X band). We can imagine an ESR experiment either by changing the Klystron frequency until the energy quantum from the microwave matches the energy gap (equation 9) or by fixing the microwave frequency and changing the energy gap until it is equal to $h\nu$. For technological reasons the latter is more easier. The field is changed at a slow rate. When resonance occurs energy absorption from the microwave field is detected. To improve signal detection this slowly varying magnetic field is modulated by a small alternating field of frequency on the order of 100 kHz. This allows the lock-in technique to be used to detect the

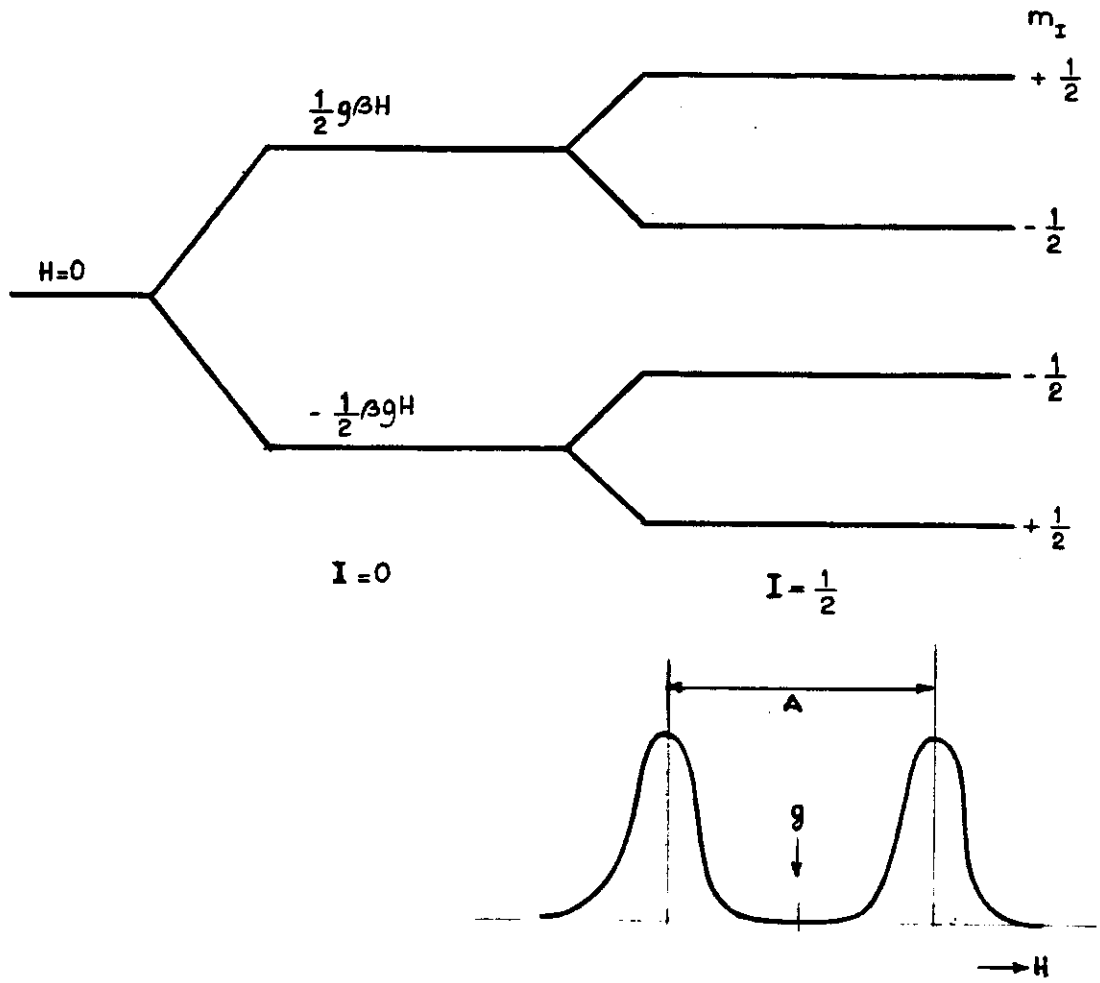

Figure 3: Energy level for a electron interacting with a nuclear spin 1/2. The absorption lines are also shown.

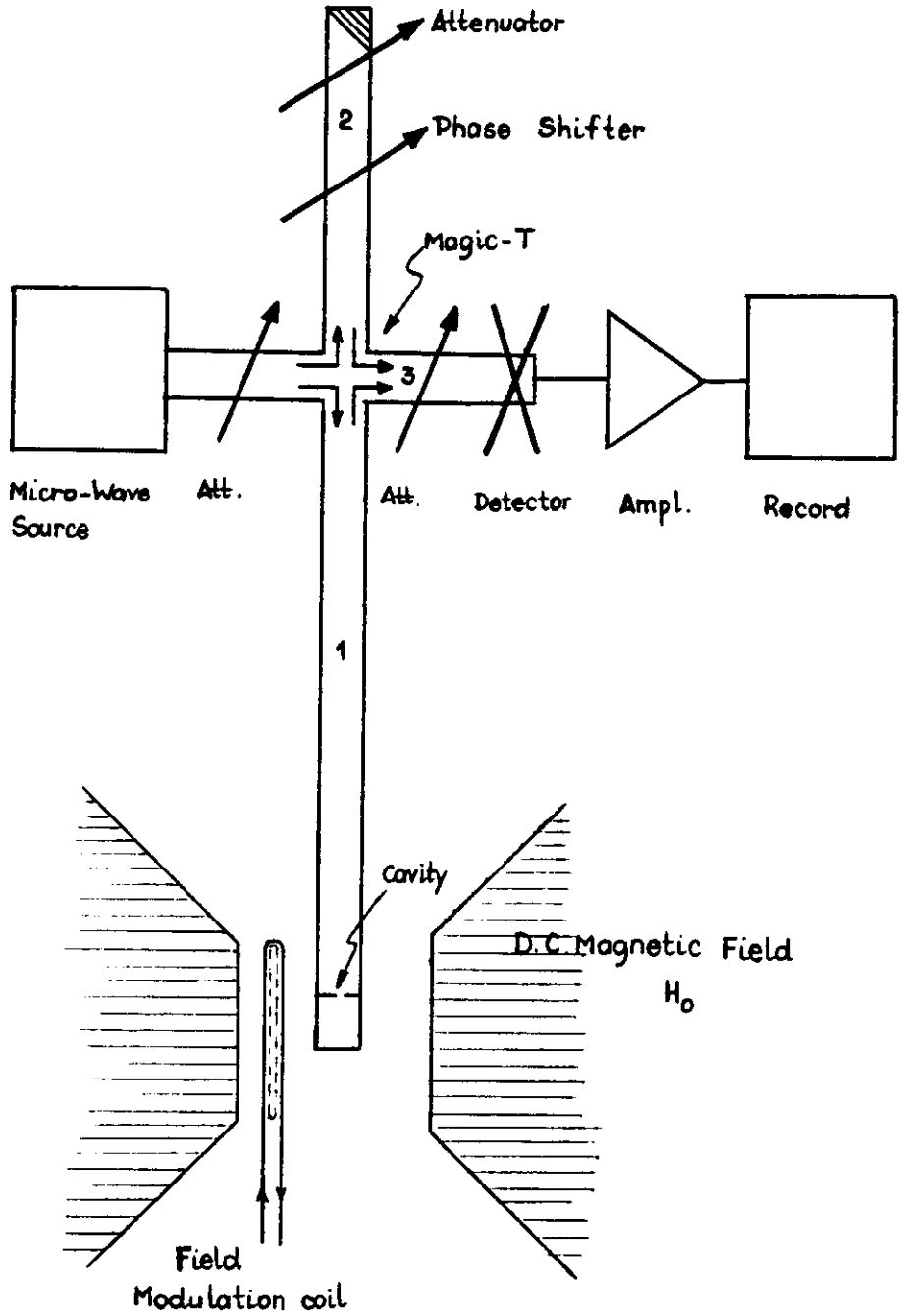

Figure 4: Block diagram of an ESR spectrometer

signal and a significant improvement in the instrumental sensitivity is obtained. When using lock-in detection the only spectral component that is detected is the one that has the same frequency as that of the modulation field. The microwave power absorption signal can be expanded as a Taylor series in the amplitude of the modulating field ΔH:

$$S = S_o + S'\Delta H + S''(\Delta H)^2 \cdots \tag{29}$$

where S_o is the signal for a constant magnetic field H_o and S'^s are derivatives relative to the modulating field. From equation 29 we see that the only term that has the same frequency as the modulating field is the second. Thus when this technique is used the first derivative of the signal is detected.

6 Quantitative ESR

To realize quantitative measurements in ESR dosimetry several factors have to be under control to guarantee reproducible measurements from sample to sample. Expression 30 shows that the signal sensitivity can be written as a function of the incident power P, the amplifier bandwidth $\Delta\nu$, the quality factor Q and the filling factor η,among other factors.

$$S = \frac{2P\chi''^2 Q_o^2 \eta^2 \pi^2}{\Delta\nu} \tag{30}$$

To increase the sensitivity we want to work at the highest possible microwave power. However care must be taken to avoid saturation. So before any systematic measurement is started a saturation curve has to be taken in order to know the maximum working microwave power. Modulation field is another concern and we should not overmodulate if we want to correlate the peak to peak first derivative intensity with the spin concentration. Only when modulation is small compared with the linewidth is there a proportionality between these quantities.

The Q and η factor are influenced by the interaction of the sample with the microwave field inside the resonant cavity. There are no knobs to turn to adjust these two factors and we should take care that: sample preparation, humidity, packing, positioning and size are as reproducible as possible from sample to sample. One way to correct for variation in these parameter is to use a secondary standard. The best is to have a reference sample inside the cavity, with g factor apart from the one we are interested, so there is no overlapping of spectral features. In this way change in one of the parameters before mentioned that affects the signal intensity can be normalized by the intensity of the standard signal. Usually Ruby is a good standard for ESR dosimetry, the Cr^{+3} in a matrix of Al_2O_3 has a g=3.140 which signal lies far way from the free radical signal.

7 Nuclear Magnetic Resonance

As far as theory is concerned the description for ESR in the previous sections can be applied to the understanding of the NMR phenomenon just by considering the appropriate constants for nuclei instead of electrons. Magnetic Resonance Imaging (MRI) will be the subject of other lectures in this college and here only a few points necessary to the understanding of MAGDOS will be stressed. Namely, how the relaxation times T_1 and T_2 can be changed.

8 Mechanisms that influence T_1 and T_2

The local field experienced by one proton in a molecule is the summation of the laboratory field and the magnetic fields produced by the neighboring nuclei. Since this molecule is in motion the fields produced by the nearby protons are fluctuating. Usually a molecule will move in a random fashion and one way to describe this motion is to suppose that the molecule stays still for a time τ_c, known as correlation rotation time, and then collides with another molecule changing its orientation. A Fourier analysis of this kind of random motion can give spectral contributions with frequencies starting from 0 to $1/\tau_c$ Hz. If the resonant frequency ω_o is in this interval a transition can be induced by this random motion. In general there is a compromise between the amount of power in this kind of motion and its range of frequencies. The wider the range less intense will be the Fourier components. The spectral density function describes how the power will change with the frequency. One way to influence the shape of the spectral function is by changing the viscosity of the medium, changing in this way the correlation time τ_c. This can be accomplished by temperature changes.

The dipole–dipole is the most important interaction in this process, and it can be modulated by changing the intensities and/or number of interacting dipoles. The importance of employing paramagnetic impurities to affect the relaxation times is immediately recognized since the γ_e for electrons is 657 times stronger than γ_I for protons. The influence of paramagnetic impurities on the relaxation times was studied by Bloembergen and others[11,8], expression 31 shows the relevant parameters affecting T_1:

$$\Delta\left(\frac{1}{T_1}\right) = \frac{12\pi^2\gamma^2\eta\mu^2 N}{5kT} \tag{31}$$

where η is the viscosity,N is the number of paramagnetic ions per unity volume, μ the magnetic moment and γ the gyromagnetic ratio.

The brightness of a MRI image pixel will depend on several factors. Two common ways to excite the sample and get the desired information is by the spin-echo and inversion-recovery pulse sequences. The intensity of the signal will be given as follows [33] :

$$I(SE) = N|1 - \exp(T_E - TR)/T_1|\exp(-T_E/T_2) \quad (32)$$

$$I(IR) = N|1 - (2 - \exp(T_E + T_I - T_R)/T_1 \exp(T_I/T_1)|\exp(-T_E/T_2) \quad (33)$$

where T_E is the time to echo, T_I is the inversion time, N is the spin concentration at the image pixel and T_1 and T_2 are relaxation times. From expressions 32 33 it can be seen that the signal intensity will depend on the relaxation times T_1 and T_2. If a way could be found to change these parameters by means of irradiation a new route to investigate the interaction of radiation with matter could be followed.

9 Examples

In this section an overview of ESR dosimetry will be given. This technique has been applied to dose assessment for a wide range of materials such as minerals, fossils, amino acids, cloth, etc. We will group the studies by the type of material utilized, since their ESR signals are similar. The method consists of measuring the concentration of spins in a given sample that has been exposed to radiation and then calibrate the material by additional irradiation with known doses in the laboratory, to assess the sensitivity to a specific kind of radiation. As pointed out previously careful measurements have to be done to find reliable spin concentrations. From the spin concentration data a fitting can be made to derive the relevant quantities such as sensitivity (slope of the curve) and the previous dose or total dose (TD) the sample received during the past.

HYDROXYAPATITE

Hydroxyapatite (HA) and collagen are the main constituents of bone. HA is the mineral content of bones and teeth, it can change in bones due to growth or demineralization but, supposedly, it does not change appreciably in tooth enamel.

Ionizing radiation can produce stable paramagnetic centers in the mineral matrix that can be used for dosimetric purposes. These centers have been found in fossil samples 10^6 years old. The paramagnetic center formed in HA is the CO_3^{3-} radical trapped in the mineral matrix. This radical has been extensive studied by Cevc,Tochon and Doi [13,18,54]. Doi et al. made a comparison of the ESR signal produced by X-rays in bone, enamel and HA doped with carbonate,leading to the conclusion that the paramagnetic center created by radiation in bone and enamel is indeed the CO_3^{3-}. The signal exhibits axial symmetry with the g values $g_\perp = 2.0025$ and $g_\parallel = 1.997$, as shown in figure 5.

The symmetry of this center was studied by making measurements at Q band frequencies at different angles of the sample relative to the magnetic field. The results indicate that there is a preferential orientation along the bone axis as shown by the graph in figure 6. Collagen also give a broad unstable signal, not good for dosimetric purposes. Heating at 70° during 10 minutes is enough to quench this signal. Figure 5 shows a typical ESR spectrum of bone (bovine tibia) irradiated with 50 Gy, Co^{60} γ rays after heat treatment.

Several authors [10,35,31] [17,14,29,40] have pointed out theimportance of this radical in the case of personal accident dosimetry or for the determination of the radiation exposure history to the exposure of low level radiation. Some of the survivors of the atomic bomb explosion in Japan have had their dose estimated by this method with quite good results [35,27]. Caracelli et al. [14] made a study to obtain the sensitivity of bone as a dosimeter. The minimum dose that can be detected is 0.5 Gy for γ rays from a Co^{60} source according to these authors. Figure 7 shows the calibration curve obtained for different irradiation sources in the dose range from 0 to 30 Gy.

The ESR dosimetry using this radical has been useful also for dating purposes [29,3,36] of human or animal remains. Figure 8 shows a typical ESR first derivative spectrum of a piece of human skull that was buried in the soil for approximately 5 thousands years. The signal is composite showing the superposition of the free radical signal produced in the mineral part and the Mn^{2+} sextet due to the absorption of manganese from the soil. This is possible because bone is very porous and behaves like an open system. The CO_3^{3-} signal is shown in figure 9 for the same sample before and after irradiation. Figure 10 shows the growth curve of the signal intensity I as a function of the dose. Extrapolation to zero ESR signal intensity gives the total dose (TD) the sample had received. If the annual dose rate is known where the sample was found the age of the sample can be determined.

ALANINE

Effects of radiation on proteins and amino acids were first studied by GORDY et al.[24]. Alanine was further studied by this group [37] and the spin Hamiltonian was determined. It was found that the radical formed is of the form $CH_3\dot{C}HR$, where R is a group that has no detectable magnetic influence. The hydrogens of the methyl group CH_3 have an isotropic hyperfine interaction of 26 G and that of the CH group is isotropic with 20 G amplitude and anisotropic with 7 G amplitude. Figure 11 shows the ESR spectrum of this radical and a calibration curve. Usually the peak to peak amplitude is correlated with the dose received by the dosimeter, and the results agree well with the double integration of the spectrum when made simultaneously. This dosimeter has reached a stage of practical use both for gamma rays[15,55,44,45] [6,7], electrons[49] and

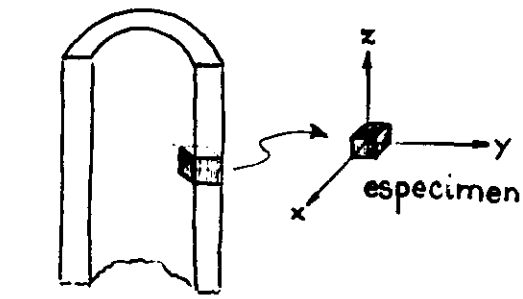

bovine tibia

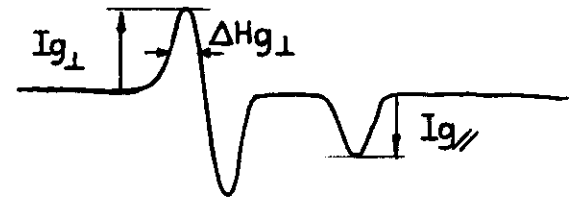

typical Q-band ESR signal

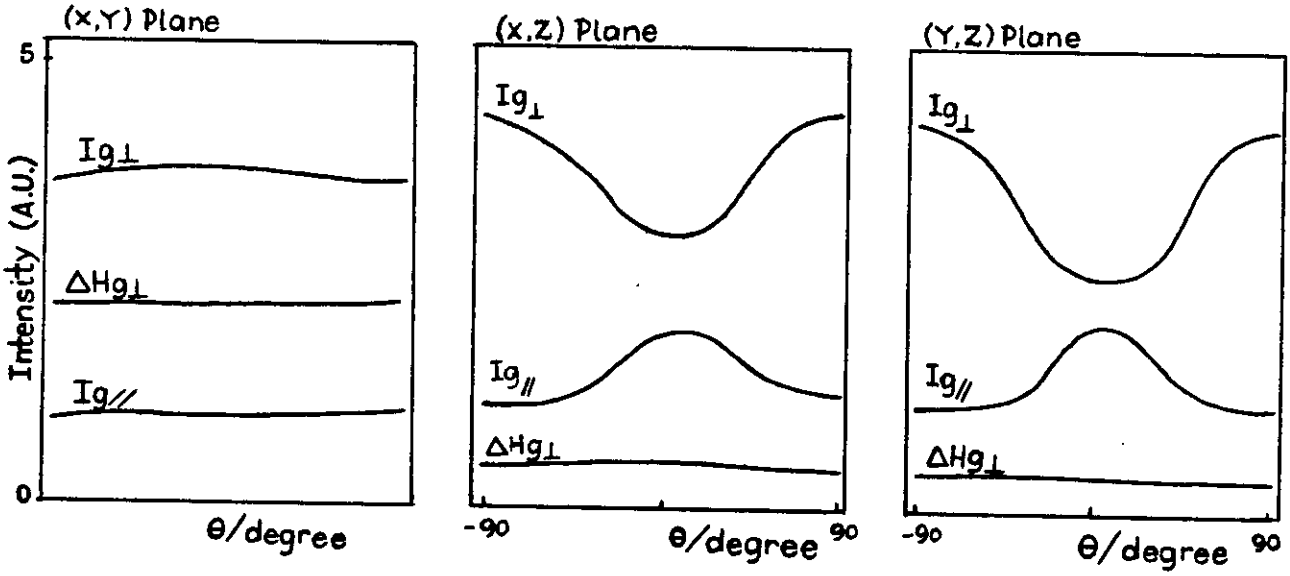

Figure 5: ESR signal intensity produced in bone as a function of the sample orientation in the magnetic field

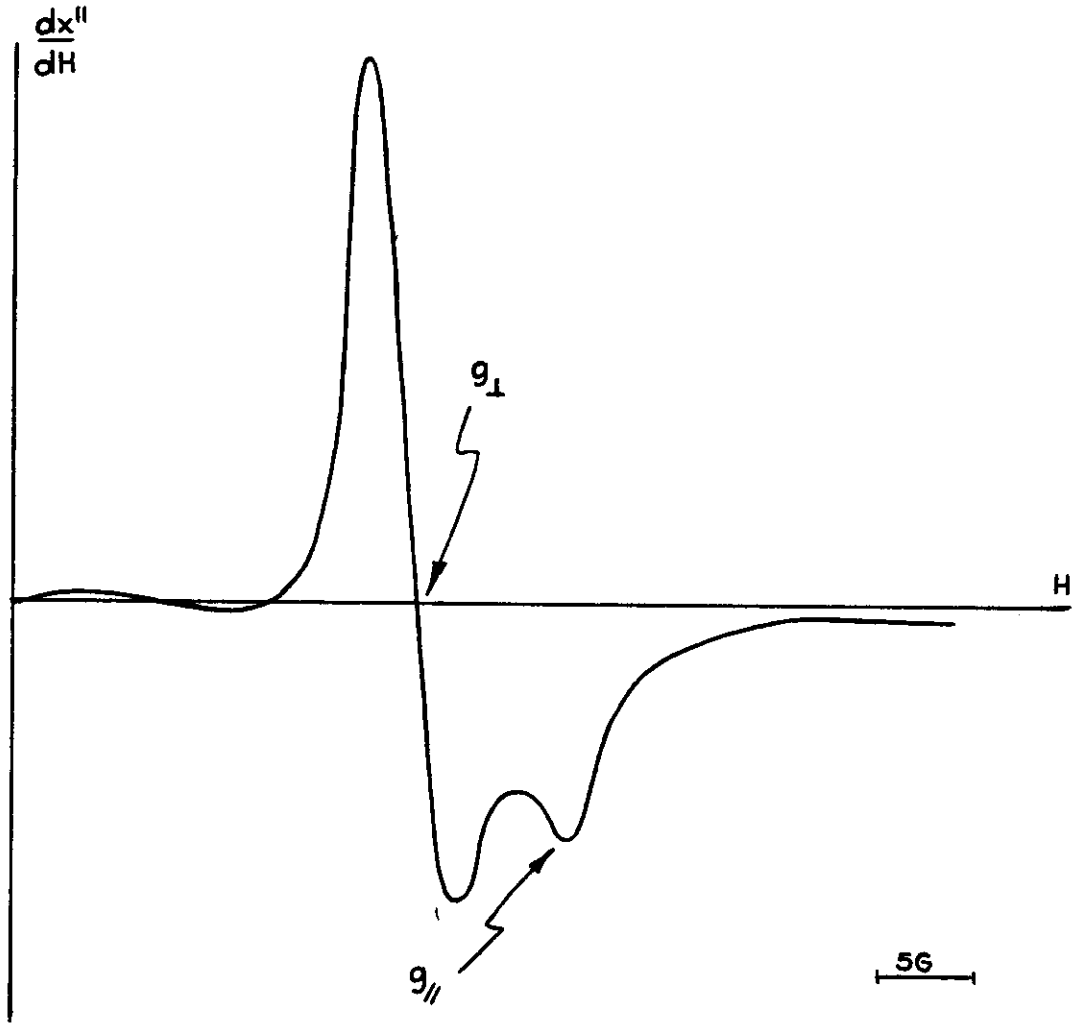

Figure 6: ESR spectrum of a bone sample irradiated with γ rays, from reference 14.

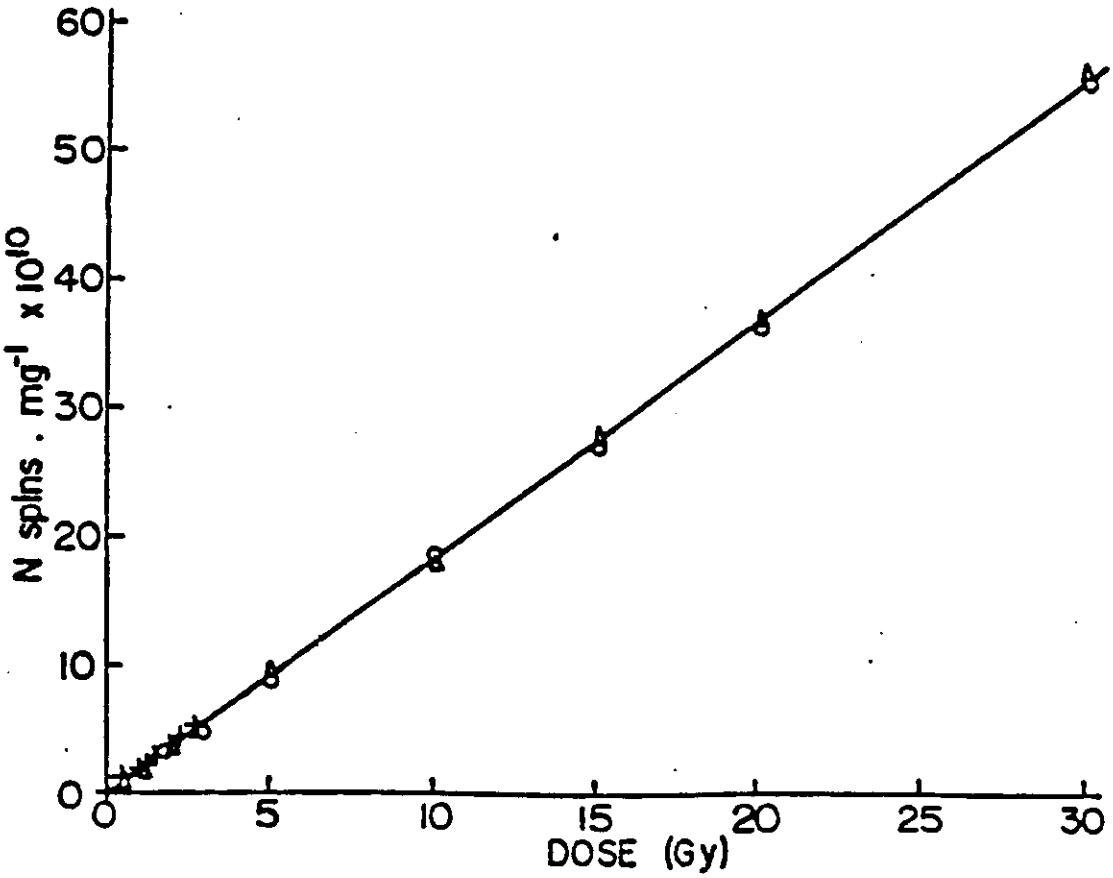

Figure 7: Spin concentration in bone a sample as a function of the dose from Co^{60} γ rays. Different symbols indicate irradiation made at different radiation facilities, data from reference 14.

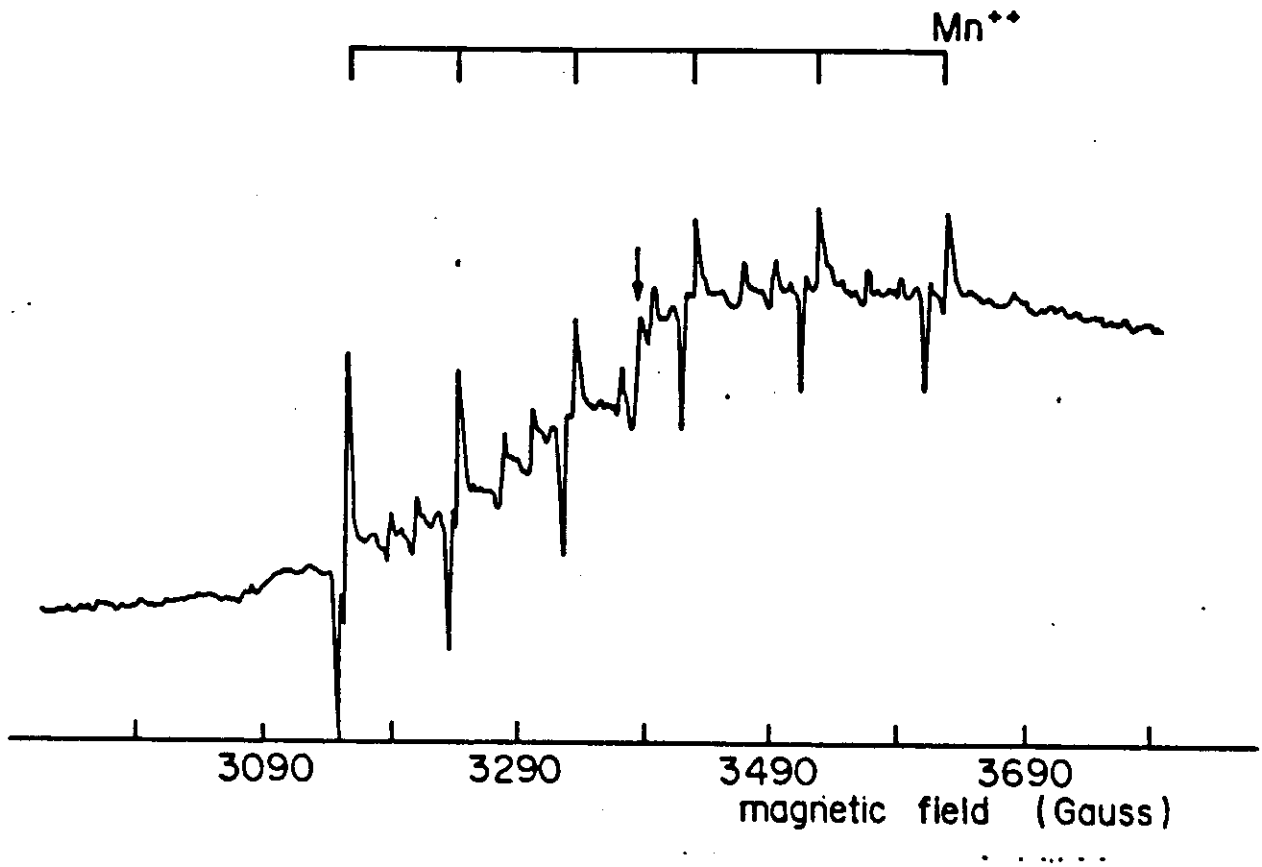

Figure 8: ESR signal of a fossil piece of skull, from reference 36.

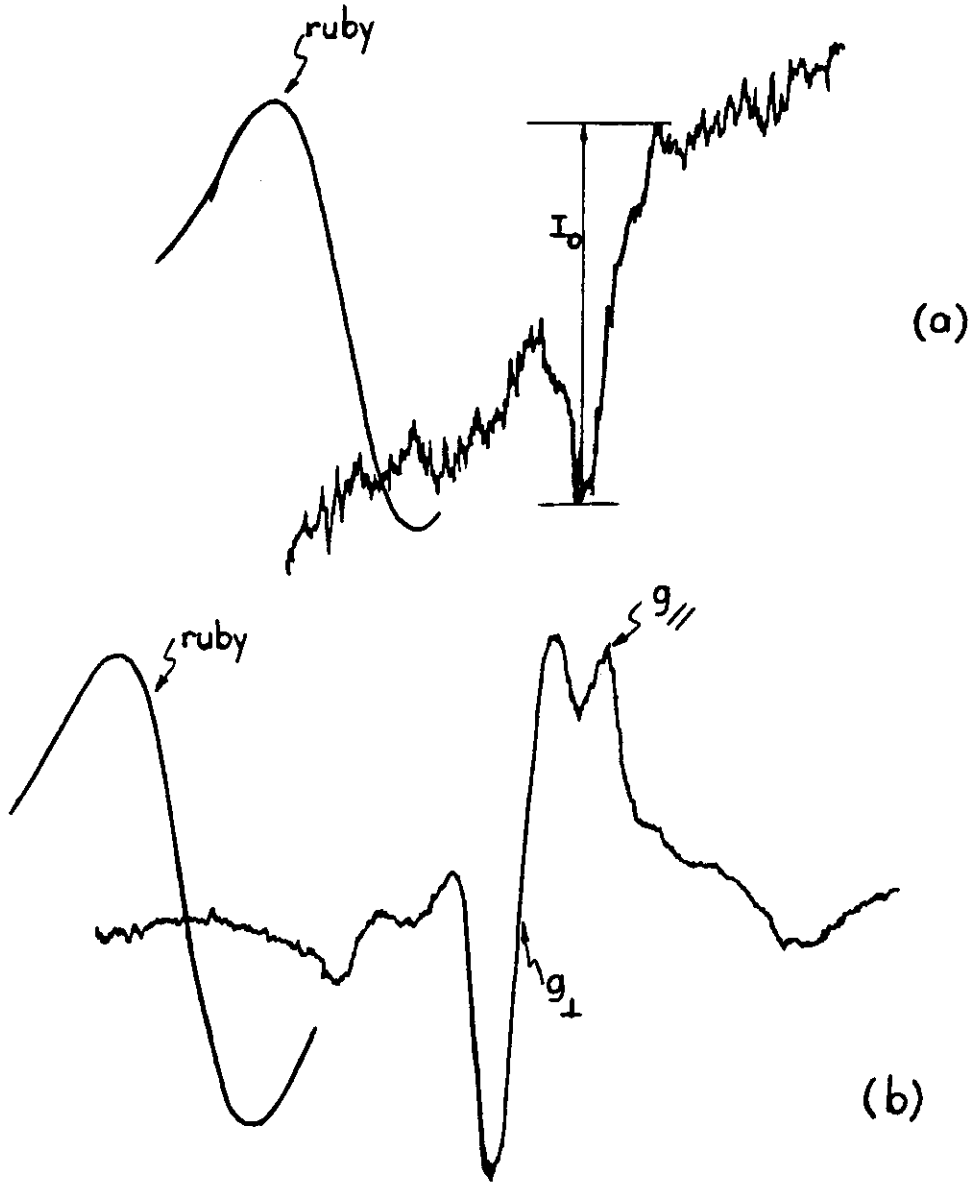

Figure 9: The ESR signal before (a) and after (b) Co^{60} irradiation, from reference 35

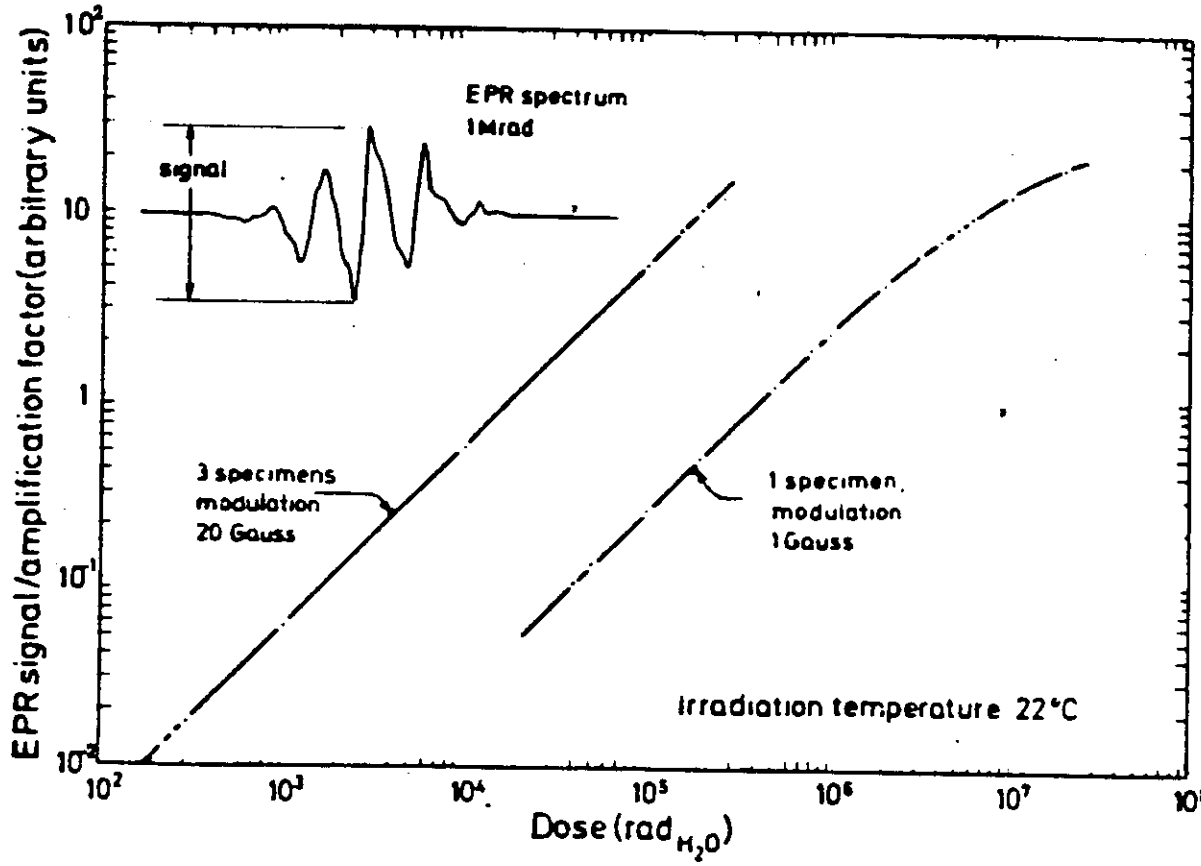

Figure 10: Typical ESR signal of alanine irradiated with γrays, from reference 45.

fast neutrons[50]. The technical aspects and progress with this kind of dosimetry were also reviewed by Regulla et al.[43,46]. Usually the alanine crystals are embedded in paraffin and pressed into a small cylinder. Recently [32] it was proposed the use of polystyrene as a binder in the preparation of this dosimeter.

NMR DOSIMETRY

The idea of NMR dosimetry is to combine the recently developed Magnetic Resonance Imagining (MRI) technique to give information about spatial distribution of dose. Thus if an image can be produced contrasted by a property that results from the interaction of radiation with matter a correspondence can be made between the MRI signal intensity and the dose delivered at a certain position. This can be very useful especially in cases where a complex radiotherapy treatment needs to be checked. Since MRI scanners are used primarily to diagnose pathologies a superposition of the region of interest in the patient and a dose MRI images in the phantom could be made to verify that the treatment planning was accurate.

The interaction of ionizing radiation with matter can produce effects that alter the proton relaxation times T_1 and T_2. As said before if the viscosity of the medium is changed, the tumbling rate of the molecules will be modified and consequently T_1 and T_2 . A viscosity dosimeter was proposed by Boni [5] based on the degradation of a polyacrylamide gel. The viscosity was measured as a function of the dose for X and γ radiation with good sensitivity in the range between 0.5–75 Gy. A phantom of this material can be made to reflect the dose distribution as a function of changes in relaxation times due to viscosity changes. However the data reported in [5] shows that the viscosity corresponding to high dose is very low. Therefore a new range of polymer concentration has to be studied that will give viscosity dose alteration and still retain information regarding the position at which the dose was delivered.

Another way to alter T_1 and T_2 is by the introduction of paramagnetic impurities in the medium. Expression 31 gather the factors that modify the relaxation time T_1 due to the presence of a paramagnetic species. The transition metal ions have a strong magnetic moment and are very effective in influencing T_1. Both Fe^{2+} and Fe^{3+} are paramagnetic species that can strongly shorten the relaxation times of water. The trivalent ion is more effective than the divalent ion owing to its magnetic moment and to the electron spin relaxation time that enhances by thirty times the correlation rotation time of the Fe^{3+} compared with that of the Fe^{2+}. That the iron behaves in this way is very fortuitous because the Fricke dosimetry is based on the $Fe^{2+} \longrightarrow Fe^{3+}$. Gore et al. [23] studied the variation of T_1 of a Fricke solution in the range of 0 to 50 Gy (figure 11) and obtained images of test tubes containing irradiated solutions.

Appleby et al. [2] have produced phantoms based on agarose gels containing

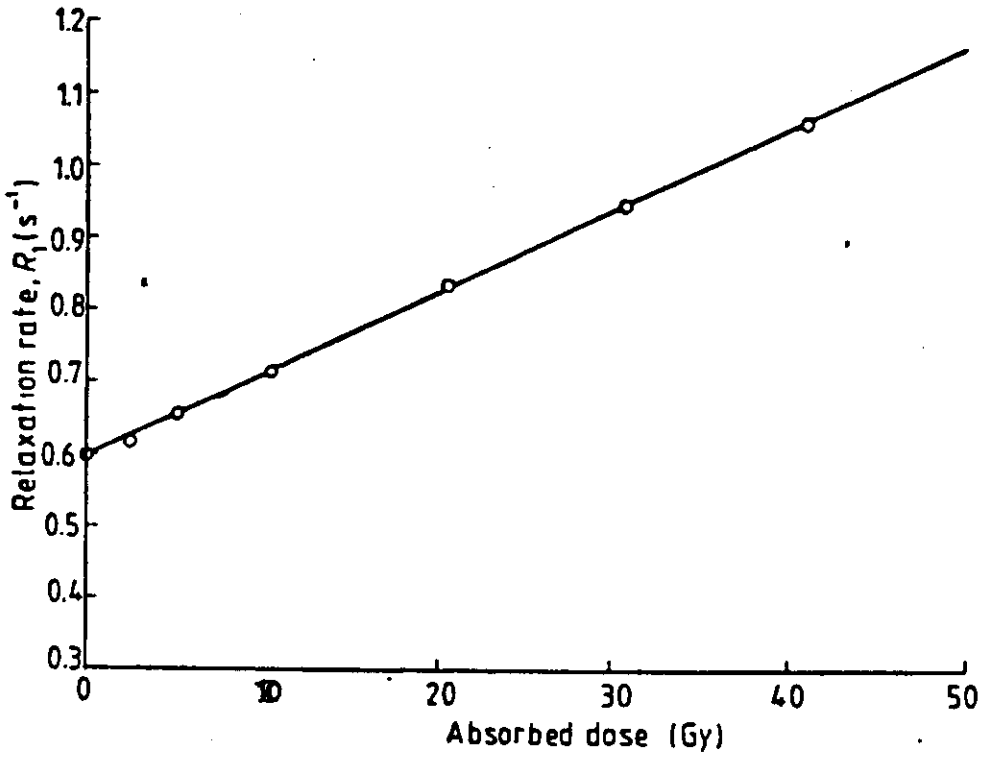

Figure 11: Relaxation rates T_1^{-1} for a ferrous sulfate solution as a function of the dose, from reference 23.

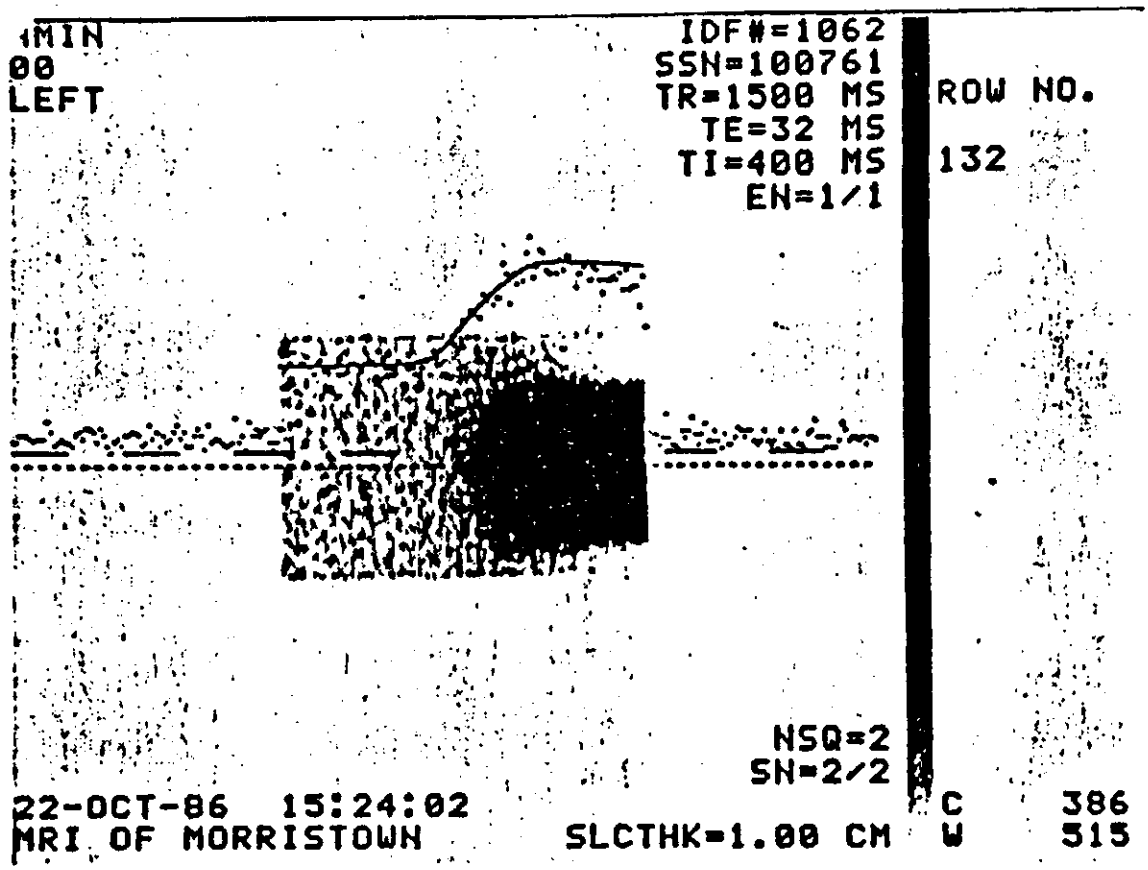

Figure 12: MRI of a agarose phantom containing ferrous sulfate solution. The maximum dose is 10 Gy.

Fricke solution that have been irradiated with γ rays and a 6–14 Mev electron beam. In figure 12 a profile of the dose produced by a 14 Mev electron beam is shown, The solid line is the dose obtained with an ionization chamber. Another candidate which produce a dose MRI phantom is the addition of spin trapping molecules to agarose gel. The radicals produced by radiation will be stabilized in a nitroxide that will change the relaxation time T_1 [12] of some portions the gel.

At least one report [47] has been published in which a decrease of T_1 was noticed in rat brain tissue that was irradiated *in vivo* with a helium beam.

There are a few points, among many, such as: stability of the phantom, diffusion of the paramagnetic species towards the low density region of this species that deserves more attention in this kind of dosimetry.

OTHER MATERIALS

Other materials such as clothing[30], organic molecules [39,56], dental restorative resins [34], carbonates [28,52] and nitroglycerol [48] have been cited in the literature as ESR dosimeters. Other citations where ESR was used in conjuction with thermoluminescence or other classical dosimetric procedure are also listed in the references.

References

[1] Aldrich J.E. and Pass B. 1986. Dental enamel as an "in vivo" radiation dosemeter: separation of the diagnostic X-ray dose from the dose due to natural sources. VIII Int. Conf. on Solid State Dosim. Oxford, England. Radiat. Prot. Dosim. (GB) 17(1-4) 175-179.

[2] Appleby, A.,Christman, E.A. and Leghrouz, A. 1987. Imaging of spatial radiation dose distribution in agarose gels using magnetic resonance. Med. Phys. 14(3), 382-384.

[3] Baffa O. and Mascarenhas S. 1985. ESR Dating of Shells from Sambaquis (Brazilian Shell Mounds). ESR dating and Dosimetry (IONICS-Tokyo), 139-43.

[4] Baffa O. and Mascarenhas S. 1985. Radiation Quality Dependence of ESR Dating of Bones and Shells. ESR dating and Dosimetry (IONICS-Tokyo),369-72.

[5] Boni, A.L. 1961. A Polyacrylamide Gamma Dosimeter. Rad. Res. 14, 374-380.

[6] Bartolotta A., Caccia B., Indovina P.L., Onori S. and Rosati A. 1985. Applications of alanine-based dosimetry. High-Dose Dosim. Proc. Int. Symp. Vienna, Austria.

[7] Bartolotta A. and Onori S. 1986. ESR technique in radiation dosimetry. Nucl. Sci. J. (Taiwan) 23(1) 77-79.

[8] Bloembergen N. and Morgan L.O. 1961. J. Chem. Phys. 34,842.

[9] Boas J.F. 1983. Electron spin resonance and thermoluminescence in calcium oxide crystals. Proc. 7th Int. Conf. on Solid State Dosim. Ottawa, Ont., Canada. Radiat. Prot. Dosim. (GB) 6(1-4) 58-60.

[10] Brady J.M., Aarestad N.O. and Swartz H.M. 1968."In vivo" dosimetry by electron spin resonance spectroscopy. Health Phys. 15, 43-47.

[11] Brown M.A. and Johnson G.A. 1984. Transition metal-chelate complexes as relaxation modifiers in nuclear magnetic resonance. Med.Phys. 11(1), 67-72.

[12] Bryant R.G., Polnaszek C., Kennedy S., Hetzler J. and Hickerson. 1984. The magnetic field dependence of water proton T1 in aqueous solutions: implications for magnetic imaging contrast media. Med.Phys. 11(5), 712-713.

[13] Cevc P., Schara M.,Ravinik C. 1972. Electron Paramagnetic Resonance Study of Irradiated Tooth Enamel. Rad. Res. 51,581-589.

[14] Caracelli I., Terrile M.C. and Mascarenhas S. 1986. Electron spin resonance dosimetric properties of bone. Health Phys. 50(2), 259-263.

[15] Deffner U. and Regulla D.F.1980.Influences of physical parameters on high-level amino acid dosimetry. Solid State Dosim. Proc. 6th Int. Conf. Toulouse, France. Nucl.Instrum.& Methods (Netherlands) 175(1), 134-135.

[16] Desrosiers M.F. and Simic M.G. Post-irradiation dosimetry of meat by electron spin resonance spectroscopy of bones. Submitted to J. Agricultural & Food Chemistry.

[17] Duran J.E., Panzeri H. and Mascarenhas S. 1985. ESR Dating and Dosimetry (eds.) M. Ikeya and T. Miki (IONICS-Tokyo),391-6.

[18] Doi Y, Aoba T., Okazaki M., Takahashi J. and Moriwaki Y. 1979. Analysis of paramagnetic centers in X-ray-irradiated enamel, bone, and carbonate-containing hydroxyapatite by electron spin resonance spectroscopy. Calcif. Tissue Int. 28, 107-112.

[19] Dommen I.K., Sengupta S., Krishnamurthy M.V. and Mehta S.K. 1985. ESR and lyoluminescence measurements on Tris(hydroxymethyl) aminomethane. Nucl. Instrum. & Methods Phys. Res. Sect. A (Netherlands) A240(2) 406-409.

[20] Ettinger K.V., Eid A.M. and Forrester A.R. 1983. Electron spin resonance readout for LiF dosimeters. Proc. 7th Int. Conf. on Solid State Dosim. Ottawa, Ont., Canada. Radiat. Prot. Dosim. (GB) 6(1-4) 166-168.

[21] Ettinger K.V., Miola U.J., Forrester A.R. and Ghosh A. 1984. Spatial distribution of free radicals produced by neutrons. Fifth Symp. on Neutron Dosim. Proc. (EUR 9762 EN). Comm. Eur. Commumities USDOE 1985 Munich-Neuherberg, Germany.

[22] Farrar,T.C. 1987. An Introduction to Pulse NMR Spectroscopy. Farragut Press, Madison, WI.

[23] Gore, J.C., Kang, Y.S. and Schulz, R.J. 1984. Measurement of Radiation Dose distributions by Nuclear Magnetic Resonance (NMR) Imaging. Phys. Med. Biol. 29(10),1189–1197.

[24] Gordy W., Ard W.B. and Shields H. 1955. Microwave spectroscopy of biological substances. I paramagnetic resonance in X-irradiated amino acids and proteins. Phys. Duke University, North Carolina.

[25] Hansen J.W. and Olsen K.J. 1986. Detection of low and high-LET radiation with alanine. Int. J. Radiat. Appl. Instrum. Part C. Radiat. Phys. & Chem. 28(5-6) 535.

[26] Huzimura R., Asaki K. and Takenaga M. 1980. An ESR study of thermoluminescent processes in $CaSO_4$ phosphors. Solid State Dosim. Proc. 6th Int. Conf. Toulouse, France. Nucl. Instrum. & Methods (Netherlands) 175(1) 8-9.

[27] Ikeya M., Miyajima J. and Okajima S. 1984. ESR dosimetry for atomic bomb survivors using shell buttons and tooth enamel. Jpn. J. Appl. Phys. 2 (Japan) 23(9) L697-L699.

[28] Ikeya M.,Baffa Filho O. and Mascarenhas S. 1984. ESR Dating of Cave Deposits from Akiyoshi-do Cave in Japan and Diabo Cavern in Brazil. J. Spelol. Soc. Japan 9,58-67.

[29] Ikeya,M. 1988 Dating and Radiation Dosimetry with Electron Spin Resonance. Magn. Res. Review 13,91-134.

[30] Kamenopoulou V., Barthe J., Hickman C., Portal G.1986. Accidental gamma irradiation dosimetry using clothing. Radiat. Prot. Dosim. 17, 185-188.

[31] Koberle G., Terrile C., Panepucci H.C. and Mascarenhas S. 1973. On the Paramagnetism of Bone Irradiated in Vivo An. Acad. Bras. Cienc. 45(1), 157-160.

[32] Kojima T., Tanaka R., Morita Y. and Seguchi T. 1986. Alanine dosimeters using polymers as binders. Appl. Radiat. Isot. 37(6) 517-520.

[33] Mansfield P. and Morris P.G. 1982. NMR Imaging in Biomedicine. Academic Press.

[34] Marcia-Langel, M.C. and Louro S.R.W. 1986. High-level dosimetry by radiation induced free radicals in dental restorative resins. Nucl.Instrum. & Methods Phys. Res. Sect. (Netherlands) B16(4-5) 419-423.

[35] Mascarenhas S., Hasegawa A. and Takeshita K. 1973. EPR dosimetry of bones from the hiroshima A-bomb site. Bull. Amer. Phys. Soc.18,579.

[36] Mascarenhas S.,Baffa Filho O. and Ikeya M. 1982. Electron Spin Resonance Dating of Human Bones from Brazilian Shell Mounds (Sambaquis). Am. J. Phys. Anthropol. 59,413-17.

[37] Miyagawa I. and Gordy W. 1960. Electron spin resonance of an irradiated single crystal of alanine: second-order effects in free radical resonances. J. Chem. Phys. 32(1), 255-263.

[38] Moriarty T.F., Oduko J.M. and Spyrou N.M. 1988.Thermoluminescence in irradiated foodstuffs. Nature 332(3), 22.

[39] Oommen I.K., Sengupta S., Krishnamurthy M.V. and Mehta S.K. 1985. ESR and lyoluminescence measurements on tris (hydroxymethyl) aminomethane. Nucl. Instrum. Meth. Phys. Res. A240, 406-409.

[40] Pass B. and Aldrich J.E. 1985. Dental enamel as an "in vivo" radiation dosimeter. Med.Phys. 12(3), 305-307.

[41] Pake,G.E. 1962.Paramagnetic Resonance. Benjamin,Inc. New York.

[42] Poole, C.P. and Farach, H. 1976. Teoria de la Resonancia Magnetica. Editorial Reverte, S.A. Barcelona.

[43] Regulla D.F. and Deffner U. 1985. Progress in alanine/ESR transfer dosimetry. High-Dose Dosim. Proc. Int. Symp. Vienna, Austria.

[44] Regulla D.F. and Deffner U. 1982. Dosimetry by ESR spectroscopy of alanine. Int. J. Appl. Radiat. & Isot. (GB) 33(11), 1101-1114.

[45] Regulla D.F., Deffner U. and Tuschy H. 1981. A practical high- level dose meter based on tissue-equivalent alanine. IAEA Technical Report 205, 129-151.

[46] Regulla D.F. and Deffner U. 1981. Standardization in high-level photon dosimetry based on ESR transfer methodology. IAEA-SM- 249/84, 391-404.

[47] Richards T. and Budinger T. 1988. NMR imaging and spectroscopy of the mammalian central nervous system after heavy ion radiation. Radiation Research 113, 79-101.

[48] Sagstuen E., Theisen H. and Henriksen T. 1983. Dosimetry by ESR spectroscopy following a radiation accident. Health Phys. (GB) 45(5) 961-968.

[49] Schneider M.K.H., Krystek M. and Schneider C.C.J. 1985. Dosimetry of electron and gamma radiation with alanine/ESR spectroscopy. High-Dose Dosim. Proc. Int. Symp. Vienna, Austria.

[50] Simmons J.A. and Bewley. 1976. The relative effectiveness of fast neutrons in creating stable free radicals. Radiation Research 65, 197-201.

[51] Slichter,C.P. 1965. Principles of Magnetic Resonance. Harper and Row, New York.

[52] Smith B.W., Smart P.L. and Symons M.C.R. A routine ESR technique for dating calcite speleothems. VIII Int. Conf. on Solid State Dosim. Oxford, England. Radiat. Prot. Dosim. (GB) 17(1-4), 241- 245.

[53] Tatsumi-Miyajima J. 1987. ESR dosimetry for atomic bomb survivors and radiologic technologists. Nucl. Instrum. & Methods Phys. Res. Sect. A (Netherlands), A257(2), 417-422.

[54] Tochon-Danguy,H. J., Geoffroy, M. and Baud, C.A. 1980 Electron Spin Resonance Study of the Effects of Carbonate Substitution in Synthetic Apatites and Apatites from Human Teeth. Archs. oral Biol. 25,357-361

[55] Wielopolski L., Maryanski M., Ciesielski B., Forman A., Reinstein L.E. and Meek A.G. 1987. Continuous three-dimensional radiation dosimetry in tissue-equivalent phantoms using electron paramagnetic resonance in L-alpha-alanine. Med.Phys. 14(4), 646-652.

[56] Zuppiroli L., Bouffard S. and Jacob J.J. 1985. Ionizing radiation dosimetry in the absorbed dose range 0.01-50 MGy based on resistance and ESR linewidth measurements of organic conducting crystals. Int. J. Appl. Radiat. & Isot. (GB) 36(11) 843-852.